Infection and Drug Resistance

Dovepress
open access to scientific and medical research

Open Access Full Text Article

ORIGINAL RESEARCH

Emergence of SARS-CoV-2 with Dual-Drug Resistant Mutations During a Long-Term Infection in a Kidney Transplant Recipient

Yoko Tanino[1,2,*], Keisuke Nishioka[1,*], Chie Yamamoto[2,*], Yohei Watanabe[1,3], Tomo Daidoji[1,4], Masataka Kawamoto[5], Sayaka Uda[6], Shoko Kirito[1], Yuta Nakagawa[2], Yu Kasamatsu[2], Yoshiyuki Kawahara[7], Yuri Sakai[7], Shuji Nobori[8], Tohru Inaba[2], Bon Ota[9], Naohisa Fujita[7], Atsushi Hoshino[10], Yoko Nukui[2], Takaaki Nakaya[1]

[1]Department of Infectious Diseases, Kyoto Prefectural University of Medicine, Kyoto, Japan; [2]Department of Infection Control and Laboratory Medicine, Kyoto Prefectural University of Medicine, Kyoto, Japan; [3]JST, MIRAI, Tokyo, Japan; [4]School of Veterinary Medicine, Rakuno Gakuen University, Ebetsu, Hokkaido, Japan; [5]Department of Forensics Medicine, Kyoto Prefectural University of Medicine, Kyoto, Japan; [6]Department of Pulmonary Medicine, Kyoto Prefectural University of Medicine, Kyoto, Japan; [7]Kyoto Prefectural Institute of Public Health and Environment, Kyoto, Japan; [8]Department of Organ Transplantation and General Surgery, Kyoto Prefectural University of Medicine, Kyoto, Japan; [9]Department of Emergency Medicine, Kyoto Prefectural University of Medicine, Kyoto, Japan; [10]Department of Cardiovascular Medicine, Kyoto Prefectural University of Medicine, Kyoto, Japan

*These authors contributed equally to this work

Correspondence: Takaaki Nakaya; Yohei Watanabe, Department of Infectious Diseases, Kyoto Prefectural University of Medicine, 465 Kajii-cho, Kawaramachi-Hirokoji, Kamigyo-ku, Kyoto, 602-8566, Japan, Tel +81-75-251-5325, Fax +81-75-251-5328, Email tnakaya@koto.kpu-m.ac.jp; nabe@koto.kpu-m.ac.jp

Introduction: Various therapeutic agents are being developed for the treatment of coronavirus disease 2019 (COVID-19). Therefore, it is crucial to accumulate information regarding the features of drug-resistant viruses to these antiviral drugs.

Methods: We investigated the emergence of dual-drug resistance in a kidney transplant recipient who received sotrovimab (from day 0) and remdesivir (RDV) (from day 8 to day 17). We sequenced the whole viral genomes from nasopharyngeal swabs taken on day 0 and seven points after starting treatment (on days 12, 19, 23, 37, 43, 48, and 58). The genetic traits of the wild-type (day 0) and descendant viruses (after day 12) were determined by comparing the genomes with those of a Wuhan strain and the day 0 wild-type strain, respectively. Three viral isolates (from samples collected on days 0, 23, and 37) were investigated for their escape ability and growth kinetics in vitro.

Results: The sotrovimab resistant mutation (S:E340K) and the RDV resistant mutation RdRp:V792I (nt: G15814A) emerged within 12 days (day 12) and 11 days (day 19) after the treatment, respectively. The day 23 isolate harboring S:E340K/RdRp:V791I was resistant to both sotrovimab and RDV, showing 364- and 2.73-fold higher resistance respectively, compared with the wild-type. Moreover, compared with the day 23 isolate, the day 37 isolate accumulated multiple additional mutations and had a higher level of resistance to both drugs.

Conclusion: Drug-resistant variants with double mutations (S:E340K/RdRp:V791I) became dominant within 23 days after starting treatment, suggesting that even a combination therapy involving sotrovimab and RDV, dual-drug resistant viruses may emerge rapidly in immunocompromised patients. The dual-resistant variants had lower virus yields than those of the wild-type virus in vitro, suggesting that they paid a fitness cost.

Keywords: SARS-CoV-2, sotrovimab, remdesivir, drug resistance, immunosuppression therapy

Introduction

Treatment methods for COVID-19 have been established since the pandemic was first described. Current treatments are effective in many patients; however, immunocompromised patients require long-term treatment, and emerging resistant variants occur more frequently. Resistant variants against sotrovimab, a therapeutic monoclonal antibody, have been

Received: 6 September 2023
Accepted: 22 January 2024
Published: 8 February 2024

reported during its initial administration.[1–5] Major escape amino acid mutations from sotrovimab occur at residues 337 and 340 of the spike protein in immunosuppressed patients, such as those undergoing organ transplants.[2–5] Variants resistant to RDV, an RNA-dependent RNA polymerase (RdRp) inhibitor, have a V792I mutation in nonstructural protein 12 (nsp12:RdRp) that emerged earlier than other mutations in this protein.[6]

Here, we report the accumulation of SARS-CoV-2 genome mutations within 2 months of treatment with sotrovimab and RDV infusions in a kidney transplant recipient. Amino acid mutations were evaluated at eight time points, just before the initiation of treatment (day 0) to 58 days after starting treatment, using whole-genome sequencing. We detected variants with mutations for resistance against these two drugs, E340A in the spike protein and V792I in RdRp. We also isolated viruses from nasopharyngeal swabs, and viral growth and resistance to sotrovimab or RDV were evaluated by in vitro infection assays.

Materials and Methods

Sample Donor

A 62-year-old woman presented with sore throat and fever as her chief complaints. She had a history of renal failure due to polycystic kidney disease and was a living-donor kidney transplant recipient, receiving immunosuppressive therapy with prednisolone, mycophenolate mofetil, and everolimus. Due to worsening symptoms, she was admitted to hospital 7 days after the illness onset. She was diagnosed with COVID-19 based on a positive reverse-transcription polymerase-chain reaction (RT-PCR) result for SARS-CoV-2 using a nasopharyngeal swab sample. Computed tomography revealed multiple, localized ground-glass opacities in the peripheral lung fields bilaterally. Genetic analysis revealed that SARS-CoV-2 was a Delta variant. Owing to her age and immunosuppressed status, she received sotrovimab on day 0 (the day of admission). However, her clinical condition worsened and oxygen supplementation was started on day 6 together with dexamethasone (6.6 mg/day). Furthermore, RDV was also started on day 8, and hemodialysis was started on day 9. The respiratory condition deteriorated and the patient was intubated and started on mechanical ventilation on day 13. Sputum culture taken at that time was positive for *Aspergillus niger* and *Aspergillus galactomannan* antigen in the blood. The patient was diagnosed with COVID-19-associated invasive pulmonary aspergillosis and treatment was started using voriconazole. The patient's respiratory condition subsequently improved, and she was extubated and weaned from the ventilator on day 16. RDV was discontinued after 10 days (until day 17), and dexamethasone was administered (until day 42) and then tapered. Nasopharyngeal swabs were collected from one nostril just before treatment (day 0) and on days 12, 19, 23, 37, 43, 48, 58, and 71 after treatment (Supplementary Figure 1) and stored in a viral transport medium in a 4°C refrigerator on day 1 and then stored in a −80°C freezer until testing. SARS-CoV-2 was no longer detected using real-time RT-PCR on day 71, remaining undetected the next day. The patient was discharged from hospital on day 84.

Cell Culture and Viral Isolation

VeroE6/TMPRSS2 cells (JCRB Cell Bank: JCRB1819) and a Calu-3 human lung cell line (ATCC HTB-55) were cultured and maintained in DMEM supplemented with 10% fetal bovine serum (FBS), 100 U/mL penicillin, 100 μg/mL streptomycin, and 250 ng/mL amphotericin B. Each nasopharyngeal swab was filtered using a 0.45 μm membrane filter, and then adsorbed onto VeroE6/TMPRSS2 cells to isolate the virus for virological use as described below.

RNA Extraction and Real-Time PCR

The diagnosis of COVID-19 was confirmed by PCR testing. Briefly, total RNA was extracted from a 0.25 mL nasopharyngeal swab sample (days 12, 19, 23, 37, 43, 48, 58, and 71) using TRIzol LS reagent and the PureLink RNA Mini kit (Thermo Fisher Scientific, MA, USA), according to the manufacturer's protocols. The extracted RNA was then amplified using real-time RT-PCR using the COBAS SARS-CoV-2 kit and the COBAS 6800 system (Roche, Basel, Switzerland) to quantify the cycle threshold (Ct) value.

Viral Genome Sequencing and Alignment Analysis

For SARS-CoV-2 genotyping, whole-viral genome sequences extracted from nasopharyngeal swab samples (on days 0, 12, 19, 23, 37, 43, 48, and 58) were determined using the MinIon Mk1C next-generation sequencer (Oxford Nanopore Technologies, Oxford, UK). Library preparation was performed using the NEBNext ARTIC SARS-CoV-2 Companion kit (New England Biolabs, MA, USA) and sequencing was performed according to the manual of the National Institute of Infectious Diseases (https://www.niid.go.jp/niid/images/lab-manual/SARS-CoV2_genome_analysis_manual_Nanopore_NEB_ver_1_6_220127.pdf). Sequence data were obtained for each sample. Aligning each read to the SARS-CoV-2 Wuhan strain sequence (NC_045512.2) was performed using NanoPipe,[7] and consensus sequences were obtained for each sample. Mutations in the whole viral genome were detected by NextClade (https://clades.nextstrain.org/) using each consensus sequence.

Growth Kinetics of Isolated Viruses

Whole-viral genome sequencing revealed that mutations accumulated between days 23 and 37; therefore, virus isolates from nasopharyngeal swab on days 0, 23 and 37 (named vD0, vD23, and vD37, respectively) were used for further virological analysis in this study. The virus titration was performed by measuring focus-forming units (FFU) in focus-forming assays on VeroE6/TMPRSS2 cells.[8] Calu-3 cells without air–liquid interface conditions were the infected with the three isolates at a multiplicity of infection of 0.001. After adsorption for 1 h, the cells were washed twice, maintained in DMEM/F-12 medium containing 0.2% bovine serum albumin, and incubated at 37°C. Supernatants were collected at the same infected wells at each time post-infection, and progeny virus titers were determined using focus-forming assays, as described above.

Focus Reduction Neutralizing Test (FRNT)

The neutralization activities of the three isolates (vD0, vD23, and vD37) were measured using a focus reduction neutralization assay as previously described.[9] Briefly, serial dilutions of sotrovimab (starting concentration, 40,000 ng/mL) were mixed with 100 focus-forming units (FFU) of each isolate and incubated for 1 h at 37°C. The mixture was then adsorbed onto VeroE6/TMPRSS2 cells in 96-well plates for 1 h at 37°C. The cells were washed to remove inoculum and overlaid with 1% methylcellulose in DMEM containing 0.2% bovine serum albumin. The cells were cultured for 12 h at 37°C, washed, and fixed in 4% paraformaldehyde. Immunofluorescence assays were performed with a mouse monoclonal antibody against SARS-CoV-1/2 nucleoprotein clone 1C7C7 (Sigma-Aldrich, St. Louis, MO, USA) and Alexa Fluor 488 secondary antibody. Foci were counted using an inverted fluorescence microscope (Nikon ECLIPSE Ti2 system; Tokyo, Japan). The results were expressed as the 50% focus reduction neutralization titer ($FRNT_{50}$). These values were calculated using GraphPad Prism 8 software (GraphPad Software, Boston, MA, USA).

Inhibitory Effect of Remdesivir Against SARS-CoV-2 in vitro

RDV susceptibility of the three isolates (vD0, vD23, and vD37) was determined using a previously reported focus reduction assay.[10] Equal titers of 100 FFU virus/well were adsorbed onto VeroE6/TMPRSS2 cells in 96-well plates for 1 h at 37°C. The cells were then washed and overlaid with 1% methylcellulose in culture medium containing serial dilutions of active components of RDV (GS-441524, Selleck Chemicals; Houston, USA) dissolved in dimethyl sulfoxide. The cells were cultured for 12 h at 37°C, washed and fixed using 4% paraformaldehyde. Immunofluorescence assays were performed as described above for FRNT. The results were expressed as the 50% inhibitory concentration (IC_{50}). The IC_{50} values were calculated using GraphPad Prism 8.

Deep Mutational Scanning (DMS)

Deep mutational scanning (DMS) was performed to evaluate the development of sotrovimab resistance using the receptor-binding domain (RBD) of Wuhan strain spike protein.[11] Briefly, the hemagglutinin-tagged spike protein library (residues F329 to C538) encompassing all 20 amino acid substitutions in the RBD was transfected into Expi293F cells (Thermo Fisher Scientific, Waltham, MA, USA). These library cells were infected with an ACE2-harboring green fluorescent protein (GFP)-reporter virus derived from a lentiviral vector in the presence or absence of sotrovimab. GFP-

positive cells and control GFP-negative cells were harvested by fluorescence-activated cell sorting (FACS). RNA was extracted from the harvested cells, and the genotype of one amino acid substitution-induced RBD in the library cells was determined by RNA sequencing (RNA-Seq) using the next-generation sequencer Novaseq 6000 (Illumina, CA, USA). The escape value of each amino acid substitution from sotrovimab was estimated by dividing the reads-number of GFP-positive cells by that of GFP-negative cells. Each escape value was normalized to the wild-type escape value.

Statistical Analysis

Data were expressed as the mean ± standard error of the mean (SEM). The $FRNT_{50}$ and IC_{50} values were calculated using GraphPad Prism 8 software. All statistical analyses were performed via by ANOVA with Tukey's tests using Origin 9.1 software (OriginLab Corporation, MA, USA). Results with *P*-values <0.05 were considered statistically significant.

Results

Whole Genome Analysis of SARS-CoV-2 Isolated from a Kidney Transplant Patient Identifies Multiple Mutations in S, ORF1a, ORF1b and N

Consensus viral genome sequences of the eight nasopharyngeal swabs from days 0 to 58 of treatment initiation were obtained by MinIon Mk1C sequencing. Sequencing analysis identified a SARS-CoV-2 Delta variant with L452R, T478K, D614G, and P681R mutations in the spike protein on day 0 sample compared with the Wuhan strain (NC_045512.2) (Table 1; a total of 38 amino acid differences). The infectious virus was recovered on days 0, 12, 23, 37, and 43, but not on days 19, 48, and 58. The numbers of amino acid changes in the specimens, which were commonly detected through day 37, 43, 48 and 58, were 4 in the S (I101T, D178N, E340K/A, S494P), 4 in the ORF1a (L631I (nsp2:L451L), E1209G (nsp3:E391G), R3012K (nsp4:R249K),

Table 1 Deduced Amino Acid Mutations Detected by Whole Viral Genome Sequencing

Gene	Days Since Treatment Initiation							
	0	12	19	23	37	43	48	58
S	#T19R	T19R	T19R	T19R	T19R	T19R	T19R	T19R
S	T95I	T95I	T95I	T95I	T95I	T95I	T95I	T95I
S					**I101T**	**I101T**	**I101T**	**I101T**
S	G142D	G142D	G142D	G142D	G142D	G142D	G142D	G142D
S	#E156-	E156-	E156-	E156-	E156-	E156-	E156-	E156-
S	#E157-	E157-	E157-	E157-	E157-	E157-	E157-	E157-
S					**D178N**	**D178N**	**D178N**	**D178N**
S		E340K		E340A	**E340A**	**E340A**	**E340A**	**E340A**
S	Q414R	Q414R	Q414R	Q414R	Q414R	Q414R	Q414R	Q414R
S	#L452R	L452R	L452R	L452R	L452R	L452R	L452R	L452R
S	#T478K	T478K	T478K	T478K	T478K	T478K	T478K	T478K
S					**S494P**	**S494P**	**S494P**	**S494P**
S	#D614G	D614G	D614G	D614G	D614G	D614G	D614G	D614G
S	#P681R	P681R	P681R	P681R	P681R	P681R	P681R	P681R
S	#D950N							
ORF1a	V378L	V378L	V378L	V378L	V378L	V378L	V378L	V378L
ORF1a					**L631I**	**L631I**	**L631I**	**L631I**
ORF1a					**E1209G**	**E1209G**	**E1209G**	**E1209G**
ORF1a	#A1306S	A1306S	A1306S	A1306S	A1306S	A1306S	A1306S	A1306S
ORF1a	V1750A	V1750A	V1750A	V1750A	V1750A	V1750A	V1750A	V1750A
ORF1a						E1909D		
ORF1a	#P2046L	P2046L	P2046L	P2046L	P2046L	P2046L	P2046L	P2046L
ORF1a	#P2287S	P2287S	P2287S	P2287S	P2287S	P2287S	P2287S	P2287S
ORF1a	#V2930L	V2930L	V2930L	V2930L	V2930L	V2930L	V2930L	V2930L

(*Continued*)

Table 1 (Continued).

Gene	Days Since Treatment Initiation							
	0	12	19	23	37	43	48	58
ORF1a					**R3012K**	**R3012K**	**R3012K**	**R3012K**
ORF1a	#T3255I	T3255I	T3255I	T3255I	T3255I	T3255I	T3255I	T3255I
ORF1a	D3526E	D3526E	D3526E	D3526E	D3526E	D3526E	D3526E	D3526E
ORF1a	#T3646A	T3646A	T3646A	T3646A	T3646A	T3646A	T3646A	T3646A
ORF1a				L4319F	**L4319F**	**L4319F**	**L4319F**	**L4319F**
ORF1b	#P314L	P314L	P314L	P314L	P314L	P314L	P314L	P314L
ORF1b	#G662S	G662S	G662S	G662S	G662S	G662S	G662S	G662S
ORF1b				V783I	**V783I**	**V783I**	**V783I**	**V783I**
ORF1b	#P1000L	P1000L	P1000L	P1000L	P1000L	P1000L	P1000L	P1000L
ORF1b					**R1078C**	**R1078C**	**R1078C**	**R1078C**
ORF1b					**R1502K**	**R1502K**	**R1502K**	**R1502K**
ORF1b	#A1868V	A1868V	A1868V	A1868V	A1868V	A1868V	A1868V	A1868V
ORF1b	#A1918V	A1918V	A1918V	A1918V	A1918V	A1918V	A1918V	A1918V
ORF1b					**V2287I**	**V2287I**	**V2287I**	**V2287I**
ORF3a	#S26L	S26L	S26L	S26L	S26L	S26L	S26L	S26L
ORF3a	A54S	A54S	A54S	A54S	A54S	A54S	A54S	A54S
ORF7a	#V82A	V82A	V82A	V82A	V82A	V82A	V82A	V82A
ORF7a	#T120I	T120I	T120I	T120I	T120I	T120I	T120I	T120I
ORF7b	#T40I	T40I	T40I	T40I	T40I	T40I	T40I	T40I
ORF8	P93S	P93S	P93S	P93S	P93S	P93S	P93S	P93S
ORF8	D119-	D119-	D119-	D119-	D119-	D119-	D119-	D119-
ORF8	F120-	F120-	F120-	F120-	F120-	F120-	F120-	F120-
M	#I82T	I82T	I82T	I82T	I82T	I82T	I82T	I82T
N						R10Q		
N	A90S	A90S	A90S	A90S	A90S	A90S	A90S	A90S
N					**S202N**	**S202N**	**S202N**	**S202N**
N	#R203M	R203M	R203M	R203M	R203M	R203M	R203M	R203M
N	#G215C	G215C	G215C	G215C	G215C	G215C	G215C	G215C
N	#D377Y	D377Y	D377Y	D377Y	D377Y	D377Y	D377Y	D377Y

Notes: #Shows commonly observed amino acid mutations (over 85% on GISAID) in Delta variant. Bold shows amino acid changes, which were commonly detected in the specimens through day 37, 43, 48 and 58. S: E156- and E157- and ORF8: D119- and F120- show amino acid deletions.

L4319F (nsp10:L66F)), 4 in the ORF1b (V783I (nsp12: V792I), R1078C (nsp13:R155C), R1502K (nsp13:R579K), V2287I (nsp15:V236I)), and 1 in the N (S202N) compared with the wild-type virus (day 0) (Table 1 and Supplementary Table 1). Among the mutations in the spike protein at S:I101T, S:D178N, S:E340K/A, and S:S494P, S:E340K/A and S:S494P were located in the RBD (residues R319 to P541). Further intensive analysis of sequencing data by MinIon Mk1C showed another mutant, S:E340V, in addition to S:E340K/A, in the specimens between day 12 and day 19 (Table 2). After day 23, the E340A mutation was predominant (more than 95%) with E340V detected at 4.4% on day 37 (Table 2). Conventional ABI-Sanger sequencing showed a mixed signal of residue 340 (nt:22580–22582) on days 0 to 23 (Supplementary Figure 2).

The RdRp mutation was identified as ORF1b V783I (nt: G15814A). Nsp12-16 proteins are translated as ORF1ab in SARS-CoV-2 and are subsequently generated into individual proteins by proteases. This mutation (ORF1b:V783I) is at residue 792 on nsp12 (RdRp), RdRp:V792I, was indicated as a drug-resistant mutation in COVID-19 patients after RDV administration.[6] In this study, only the wild type was detected in the specimens of day 0, before a ten-day course of RDV (from day 8 to day 17). RdRp:V792I was detected in approximately 2% and 8% of sequences on day 12 and day 19, respectively, and subsequently became dominant after day 23 (>90% of sequences, Table 2).

Table 2 Proportion of Each Variant at Each Date

Days since treatment initiation	Spike				RdRp (nsp12)		Ct value
	Wild Type (%)	Variants (%)			Wild type (%)	Variant (%)	
	S:E340	S:K340	S:A340	S:V340	RdRp:V792	RdRp:I792	
0	94.2				97.6		N/A
12		78.5	17.0	2.7	97.3	2.1	17.5
19	61.0		16.7	20.0	91.3	8.3	27.2
23			96.6		5.3	91.3	24.0
37			92.4	4.4	4.0	92.5	17.4
43			96.6			96.9	16.5
48			96.2			95.3	28.3
58			95.4			95.8	26.3
71							N.D.

Notes: The patient was treated with sotrovimab on day 0, followed by a ten-day course of RDV (from day 8 to day 17). Based on the next generation sequencing analysis of the isolated viruses (data not shown), the cutoff value was set at 2% or less. N/A shows not available. N. D. shows not detected.

In vitro Growth Kinetics of SARS-CoV-2 Variants Isolated After the Treatments

Isolates on days 23 and 37, which corresponded to time when mutations accumulated in the whole-genome sequencing, were selected for further analysis (named vD23 and vD37, respectively). The wild-type virus (vD0) was also included for comparison. The vD23 had S:E340A, ORF1a:L4319F, and RdRp:V792I mutations, whereas the vD37 further accumulated multiple mutations, especially in S, ORF1a, and ORF1b (Table 1). We investigated the replication ability of the three isolates using human lung Calu-3 cells. Both vD23 and vD37 showed less replication than vD0, with the most reduced growth observed for vD37 (Figure 1).

The Spike E340A Mutation Induced Larger Escape of SARS-CoV-2 Variants from Sotrovimab

Sotrovimab neutralized vD0 with a low $FRNT_{50}$ value (0.038 μg/mL), but showed strikingly higher, 364-fold, $FRNT_{50}$ values (13.845 ± 1.189 μg/mL and 16.803 ± 3.233 μg/mL) against vD23 and vD37, respectively (Figure 2A). The additional S:S494P mutation in the RBD of vD37 did not show a significant increase in the $FRNT_{50}$ value compared with that of vD23 (Figure 2B). To comprehensively understand the mutations escaping sotrovimab, we conducted a DMS in a region spanning residues 329 to 538 of the RBD using the inverted infection assay, where ACE2-harboring viruses

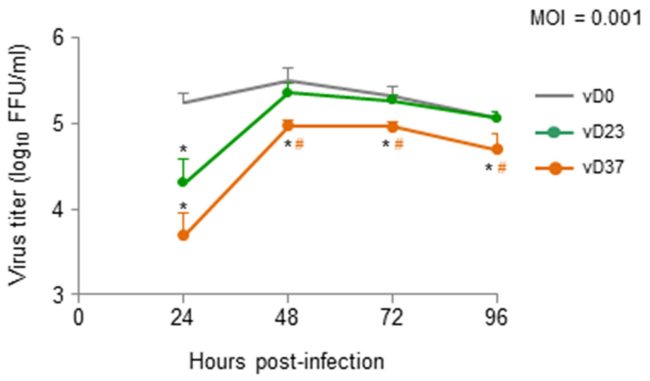

Figure 1 Isolated viruses on days 23 and 37 showed reduced replication in vitro. Three types of isolated variants were analyzed. vD0, vD23, and vD37 were isolated from nasopharyngeal swabs on days 0, 23, and 37. Calu-3 cells were infected with each variant at a multiplicity of infection of 0.001. Viral supernatant titers were determined using focus-forming assays at the indicated time points. The data represent the mean ± SEM of the three experimental replicates. Statistically significant differences compared with the virus titers of vD0 (*$P < 0.05$) and vD23 (#$P < 0.05$) were determined by analysis of variance (ANOVA) with Tukey's multiple comparison test.

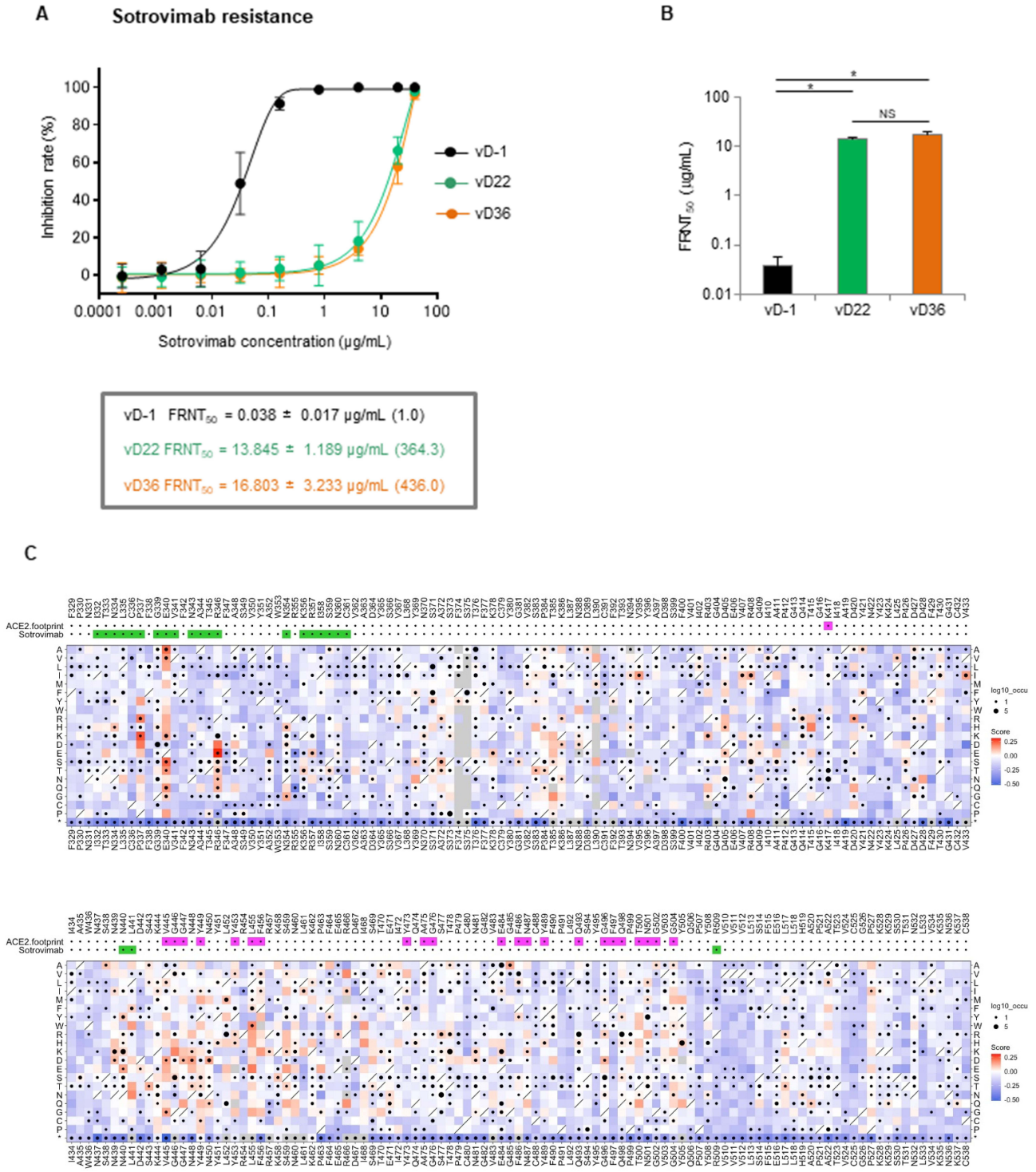

Figure 2 Isolated viruses on days 23 and 37 with the Spike E340A mutation are resistant to sotrovimab. Sotrovimab resistance was assessed using a focus reduction neutralization assay. Each diluted sotrovimab sample was mixed with 100 FFU of each variant for neutralization. After 1 h, the mixture was adsorbed onto VeroE6/TMPRSS2 cells for 12 h. (**A**) Inhibition rate from the focus numbers at the indicated sotrovimab concentration. (**B**) The 50% focus reduction neutralization titer ($FRNT_{50}$). The data represent the mean ± SEM of the three experimental replicates (*$P < 0.05$). (**C**) A deep mutational scanning (DMS) was performed in a region spanning residues 329 to 538 of the RBD using the inverted infection assay as previously described.[11] The library cells, containing the hemagglutinin-tagged RBD encompassing all 20 amino acid substitutions, were infected with an ACE2-harboring green fluorescent protein (GFP)-reporter virus derived from a lentiviral vector, both in the presence and absence of sotrovimab. Subsequently, GFP-positive cells and control GFP-negative cells were individually harvested through fluorescence-activated cell sorting. RNA was then extracted from the harvested cells for RNA-Seq, which determined the genotype of RBD induced by each amino acid substitution in the library cells. The escape value of each amino acid substitution was estimated by dividing the reads number of GFP-positive cells by that of GFP-negative cells. Log10 enrichment ratios for all individual mutations were calculated and normalized with the wild type. The heatmap illustrating how all single mutations affect the escape from sotrovimab. Squares are colored by mutational effect according to scale bars on the right, with red indicating higher escapability. Squares with a diagonal line through them indicate Wuhan strain amino acid. The black dot size reflects the frequency in the virus genome sequence according to the GISAID database as of 17th Sep 2022. ACE2 and sotrovimab footprints are highlighted in magenta and light green, respectively. Footprints on RBDs were defined according to the 5A distance from ACE2- or monoclonal antibody-contacting residues.[12]

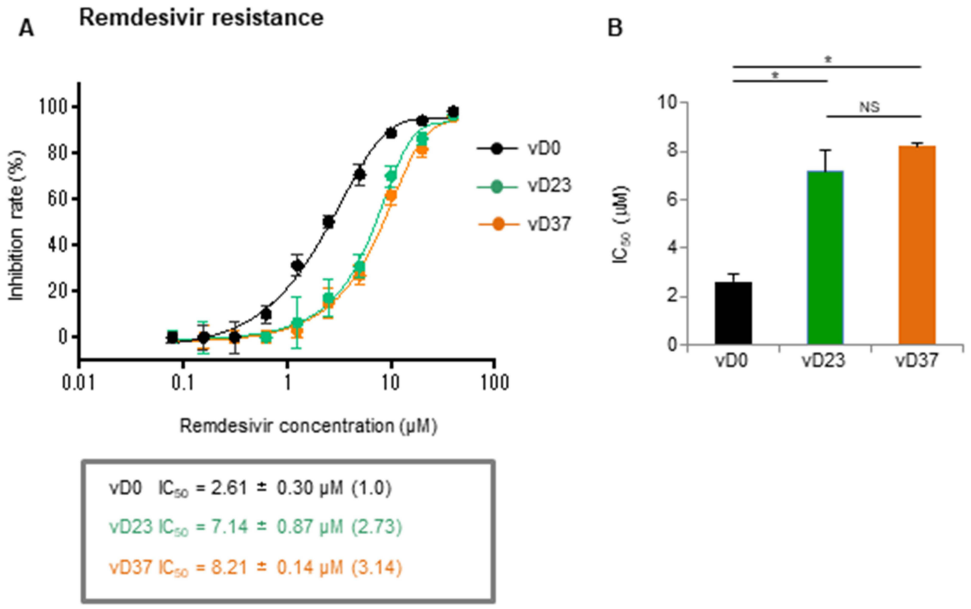

Figure 3 Isolated viruses on days 23 and 37 with the RdRp (nsp12) V792I mutation are also resistant to remdesivir. Remdesivir susceptibility was assessed using a focus reduction neutralization assay. VeroE6/TMPRSS2 cells were infected with 100 FFU of each variant and the cells were cultured in a medium containing serial dilutions of active components of remdesivir. (**A**) The focus numbers were counted, and the inhibition rate was calculated after 12 h culture. (**B**) The 50% inhibitory concentration (IC_{50}). The data represent the mean ± SEM of the three experimental replicates (*$P < 0.05$).

infected spike-expressing cells.[11] This approach can directly analyze the viral escape reflecting both alterations of antibody binding and infectivity. The result indicated that several amino acid mutations at positions 337, 340, and 346 of the spike protein-induced resistance to sotrovimab (Figure 2C and Supplementary Table 2) and within these three mutations, the first two amino acid changes have been reported as critical sites for sotrovimab resistance in vivo.[5] Among amino acid substitutions in 340 of the spike, E340A had the highest escape value (Supplementary Table 2). Majority of the spike 337 residue mutations were synonymous substitutions of P337 or had escape values lower than that of the wild-type. However, an escape value of P337R showed higher than that of the wild-type, although S:P337R mutation was not detected in this study. In addition, despite a series of comprehensive mutations at position 494, no higher escape values were observed compared with the wild-type S:S494 (Figure 2C).

The RdRp V792I Mutation Reduced Remdesivir Susceptibility of SARS-CoV-2 Variants

Next, we examined the RDV susceptibility of the three isolates (vD0, vD27, and vD37) by determining their IC_{50} values. vD23 and vD37 had higher IC_{50} values than vD0 (Figure 3A) with RDV, indicating that the both variants have reduced susceptibility to RDV. The median IC_{50} variant values were 2.61, 7.14, and 8.21 μM for vD0, vD23, and vD37, respectively. The fold changes in IC_{50} were 2.73 for vD23 and 3.14 for vD37 compared with vD0. The highest IC_{50} was observed for vD37, although there were no significant differences between vD23 and vD37 (Figure 3B). No additional mutations were detected in the RdRp (nsp12) of vD37 compared with that of vD23 (Table 1 and Supplementary Table 1).

Discussion

It has been reported that SARS-CoV-2 has acquired treatment-specific resistance mutations against antiviral drugs.[2–6] This study reported the emergence of dual-drug resistant SARS-CoV-2 variants after exposure to sotrovimab and RDV in a kidney transplant recipient. Neutralizing antibodies became detectable after sotrovimab infusion, whereas they were not detectable after SARS-CoV-2 vaccinations in the patient (data not shown). Therefore, it is likely that almost all of them might have derived from the infused sotrovimab, and they remained stable for 7 weeks after the treatment (data not

shown). Such a prolonged presence of sotrovimab may be associated with a risk for inducing drug-resistant variants and selecting the highest escape mutation in immunocompromised patients.

In this study, mutations at S:E340K/A/V were found on day 12, and S:E340K was detected 50% more frequently than S:E340A/V (as shown in Table 2). Transition mutations (purine to purine or pyrimidine to pyrimidine) are more likely than transversions (purine to pyrimidine or pyrimidine to purine); therefore, it is possible that the S:E340K transition mutation (nt:22580–22582 GAA to AAA) appeared earlier than the S:E340A and S:E340V transversion mutations (GAA to GCA and GAA to GTA) (as shown in Supplementary Table 2), consistent with a previous report demonstrating that the S:E340K mutation initially emerged in three out of four patients.[2] We previously demonstrated a DMS approach to evaluate escape from neutralizing antibodies, such as casirivimab[11] and performed a similar analysis in this study to evaluate escape mutations against sotrovimab. The S:E340A mutant showed the highest resistance to sotrovimab among the S:E340D/G/K/A/V resistant mutations previously reported in vivo according to DMS analysis (as shown in Supplementary Table 2 and Figure 2C). In addition, the isolated variants (vD23 and vD37) with the S:E340A mutation showed a > 360-fold reduction in the neutralizing activity of sotrovimab compared with that of the wild-type virus (vD0) (as shown in Figure 2A and B). Destras et al[4] indicated that the selection of sotrovimab-resistant escape variants was linked to persistent SARS-CoV-2 excretion for up to 43 days. In our case, the cycle threshold (Ct) value was still under 30 through 58 days after the sotrovimab treatment (as shown in Table 2). This may explain why the S:E340A mutant became dominant (more than 95%) 23 days after the sotrovimab treatment initiation (as shown in Table 2). DMS analysis demonstrated several other strong escape mutations, as shown in Figure 2C. These mutations involved transversion mutations or 2-base substitutions and may require caution in COVID-19 patients with longer-term infections. We also detected the S:S494P mutation after day 37; however, DMS analysis did not show significant differences in escape values against sotrovimab (as shown in Figure 2C and Supplementary Table 2). The S:S494P mutation confers reduced susceptibility to other therapeutic monoclonal antibodies such as casirivimab and bamlanivimab.[13,14] However, our neutralization analysis using sotrovimab did not show significant differences of $FRNT_{50}$ values between the isolated variants with the S:E340A (vD23) and S:E340A/S:S494P (vD37) dual mutations (as shown in Figure 2A and B).

Stevens et al[15] demonstrated that in vitro serial passage in the presence of increasing concentration of RDV (GS-4441524) led to the identification of several amino acid mutations related to RDV resistance in the RdRp, including V166A, N198S, S759A, V792I and C799F/R. Other groups identified RdRp:E802D[16] or RdRp:V166L[17] resistant mutations due to in vitro selection experiments. Among these mutations, the RdRp:V792I was detected in COVID-19 patients after RDV administration by Hogan et al.[6] The authors demonstrated that RdRp:V792I *de novo* mutation was detected 38 and 7 days after COVID-19 diagnosis following RDV treatment in two renal transplant patients. In addition, newly arising RdRp:V166L and RdRp:I536V mutations[18] and RdRp:E802D mutation[19] were found by other groups in immunocompromised patients that required RDV treatment. We detected the RdRp:V792I mutation in approximately 8% of sequences in the specimens of day 19, although only the wild type was detected on day 0, before a ten-day course of RDV (from day 8 to day 17). Interestingly, the proportion of wild-type S:E340 transiently recovered on day 19 (as shown in Table 2), which may be related to the prior administration of RDV until that point. The PCR Ct value (27.2) on day 19 was close to the maximum value (28.3) among the seven time points ranging from day 12 to day 58 (as shown in Table 2). The ratio of the RdRp:V792I mutation became dominant after day 23 (>90% of sequences, Table 2) and the S:E340A mutation also became dominant (more than 95%) in the specimen of the same day (as shown in Table 2). Sequencing analysis of the isolated variant (vD23) on day 23 confirmed that the virus had both S:E340A and RdRp:V792I mutations (data not shown). Indeed, vD23 showed a dual-resistance phenotype against sotrovimab (364-fold) and RDV (2.73-fold) (as shown in Figures 2 and 3). Thus, even a combination therapy involving sotrovimab and RDV, dual resistant mutant virus may emerge rapidly and pose a risk for both clinical and virological relapse in immunocompromised patients. In vitro viral replication analysis indicated that vD23 and vD37 had less replication than vD0, suggesting a fitness cost (as shown in Figure 1). Similar findings of RdRp:V792I mutation were reported by another group, demonstrating that mutations in the homologous site of murine hepatitis virus show resistance to RDV and reduced proliferation.[15] In addition, it has been suggested that the above RdRp:E802D mutation confers an approximately 6-fold increase in RDV IC_{50} but it also leads to a decreased viral replication relative to its parental virus in the absence of RDV.[19] Therefore, reduced replication of vD23 in this study could be due to RdRp:V792I mutation.

Additional amino acid changes of the specimens were observed on day 37 compared with those on day 23. This included L631I (nsp2:L451I), E1209G (nsp3:E391G), and R3012K (nsp4:R249K) in ORF1a, R1078C (nsp13:R155C), R1502K (nsp13:R579K), V2287I (nsp15:V236I) in ORF1b, and S202N in ORF9/N (as shown in Table 1). Some of these mutations might lead to more reduced replication of the variants (eg, vD37) in vitro (as shown in Figure 1), although it is not clear why further fitness improvement emerged in the patient. The prolonged use of steroidal anti-inflammatory drug (as shown in Supplementary Figure 1) may have contributed to it. Nsp2:L451I, nsp3:E391G, and nsp13:R155C were previously observed,[20] while other mutations in ORF1a and 1b are unreported in previous variants, including omicron BA.1 to BA.5. A recent report suggests that transmembrane nonstructural proteins (nsp) (such as nsp3 and nsp4) generate double-membrane vesicles (DMVs). Mutations in these nsps (nsp3:E391G and nsp4:R249K) might contribute to the functions of DMVs. ORF1b mutations such as nsp13 (helicase) R155C, and R579K, and nsp15 (endoRNAase) (V236I) may contribute to viral replication. The ORF9/N:S202N mutation is a mutation hotspot, although its function remains unknown.[21] ORF9/N:S202 is located in a conserved serine/arginine-rich linker region (LKR) of the N protein, and phosphorylation of residues in the serine-arginine of LKR regulates discontinuous transcription during the early stages of replication.[22] The Delta variant possesses an N:R203M mutation compared with the Wuhan variant, and the additional N:S202N variant found in this study might be related to viral replication.

Conclusions

This case reveals that dual-drug resistant viruses can emerge rapidly in immunocompromised patients treated with sotrovimab and RDV. The dual-resistant variants had lower virus yields than the wild-type virus in vitro, suggesting a fitness cost.

Ethics and Patient Consent

The transplant donor donated the kidney voluntarily and provided written informed consent, in accordance with the Declaration of Istanbul. The patient provided written informed consent for the publication of her case details. Ethical approval for this study was obtained from the Institutional Review Board of Kyoto Prefectural University of Medicine (approval numbers: ERB-C-408-2 and ERB-C-1435-3).

Acknowledgments

Yoko Tanino, Keisuke Nishioka and Chie Yamamoto are co-first authors for this work. We thank Junichi Takagi (Laboratory for Protein Synthesis and Expression, Institute for Protein Research, Osaka University, Osaka, Japan) for providing sotrovimab. We thank the staff at the Kyoto Prefectural University of Medicine and the Kyoto Prefectural Institute of Hygienic and Environmental Sciences.

Author Contributions

All authors made a significant contribution to study conceptualization, design, and execution; data acquisition, analysis, and interpretation; or in all these areas. All authors took part in drafting, revising, or critically reviewing the article; gave final approval for the version to be published; agreed on the journal to which the article has been submitted; and agreed to be accountable for aspects of the work.

Funding

This research was supported by Keisuke Nishioka (JSPS KAKENHI grant no. 20K17468, the public promoting association Asano foundation for studies on medicine), Yohei Watanabe (JST MIRAI grant no. JPMJMI22D2, JSPS KAKENHI grant no. 22H02879), Tomo Daidoji (JSPS KAKENHI grant no. 20KK0199 and 21K08510, the Takeda Science Foundation), Masataka Kawamoto (KPUM2122Fellowship), Sayaka Uda (KPUM2121Fellowship), Atsushi Hoshino (Japan Agency for Medical Research and Development, the Research Program on Emerging and Re-emerging Infectious Diseases under 21fk0108481 and 22fk0108523), Yoko Nukui (JSPS KAKENHI grant no. 19K10554), Takaaki Nakaya (JSPS KAKENHI grant no. 21H03184), and Research Support Project for Life Science and Drug Discovery (Basis for Supporting Innovative Drug Discovery and Life Science Research (BINDS)) from AMED under Grant Number JP22ama121011.

Disclosure

The authors declare no conflicts of interest in this work.

References

1. Birnie E, Biemond JJ, Appelman B, et al. Development of resistance-associated mutations after sotrovimab administration in high-risk individuals infected with the SARS-CoV-2 omicron variant. *JAMA*. 2022;328(11):1104–1107. doi:10.1001/jama.2022.13854
2. Rockett R, Basile K, Maddocks S, et al. Resistance mutations in SARS-CoV-2 Delta variant after sotrovimab use. *N Engl J Med*. 2022;386(15):1477–1479. doi:10.1056/NEJMc2120219
3. Vellas C, Tremeaux P, Del Bello A, et al. Resistance mutations in SARS-CoV-2 omicron variant in patients treated with sotrovimab. *Clin Microbiol Infect*. 2022;28(9):1297–1299. doi:10.1016/j.cmi.2022.05.002
4. Destras G, Bal A, Simon B, Lina B, Josset L. Sotrovimab drives SARS-CoV-2 omicron variant evolution in immunocompromised patients. *Lancet Microbe*. 2022;3(8):e559. doi:10.1016/S2666-5247(22)00120-3
5. Huygens S, Oude Munnink B, Gharbharan A, Koopmans M, Rijnders B. Sotrovimab resistance and viral persistence after treatment of immunocompromised patients infected with the severe acute respiratory syndrome coronavirus 2 omicron variant. *Clin Infect Dis*. 2023;76(3):e507–e509. doi:10.1093/cid/ciac601
6. Hogan JI, Duerr R, Dimartino D, et al. Remdesivir resistance in transplant recipients with persistent coronavirus disease 2019. *Clin Infect Dis*. 2023;76(2):342–345. doi:10.1093/cid/ciac769
7. Shabardina V, Kischka T, Manske F, et al. NanoPipe-A web server for nanopore MinION sequencing data analysis. *Gigascience*. 2019;8:2.
8. Hirose R, Ikegaya H, Naito Y, et al. Survival of Severe acute respiratory syndrome coronavirus 2 (SARS-CoV-2) and influenza virus on human skin: importance of hand hygiene in coronavirus disease 2019 (COVID-19). *Clin Infect Dis*. 2021;73(11):e4329–e4335. doi:10.1093/cid/ciaa1517
9. Vanderheiden A, Edara VV, Floyd K, et al. Development of a rapid focus reduction neutralization test assay for measuring SARS-CoV-2 neutralizing antibodies. *Curr Protoc Immunol*. 2020;131(1):e116. doi:10.1002/cpim.116
10. Takashita E, Yamayoshi S, Fukushi S, et al. Efficacy of antiviral agents against the omicron subvariant BA.2.75. *N Engl J Med*. 2022;387(13):1236–1238. doi:10.1056/NEJMc2209952
11. Ikemura N, Taminishi S, Inaba T, et al. An engineered ACE2 decoy neutralizes the SARS-CoV-2 omicron variant and confers protection against infection in vivo. *Sci Transl Med*. 2022;14(650):eabn7737. doi:10.1126/scitranslmed.abn7737
12. Corti D, Purcell LA, Snell G, Veesler D. Tackling COVID-19 with neutralizing monoclonal antibodies. *Cell*. 2021;184(12):3086–3108. doi:10.1016/j.cell.2021.05.005
13. Copin R, Baum A, Wloga E, et al. The monoclonal antibody combination REGEN-COV protects against SARS-CoV-2 mutational escape in preclinical and human studies. *Cell*. 2021;184(15):3949–3961 e11. doi:10.1016/j.cell.2021.06.002
14. Gottlieb RL, Nirula A, Chen P, et al. Effect of bamlanivimab as monotherapy or in combination with etesevimab on viral load in patients with mild to moderate COVID-19: a randomized clinical trial. *JAMA*. 2021;325(7):632–644. doi:10.1001/jama.2021.0202
15. Stevens LJ, Pruijssers AJ, Lee HW, et al. Mutations in the SARS-CoV-2 RNA-dependent RNA polymerase confer resistance to remdesivir by distinct mechanisms. *Sci Transl Med*. 2022;14(656):eabo0718. doi:10.1126/scitranslmed.abo0718
16. Szemiel AM, Merits A, Orton RJ, et al. In vitro selection of remdesivir resistance suggests evolutionary predictability of SARS-CoV-2. *PLoS Pathog*. 2021;17(9):e1009929. doi:10.1371/journal.ppat.1009929
17. Checkmahomed L, Carbonneau J, Du Pont V, et al. In vitro selection of remdesivir-resistant SARS-CoV-2 demonstrates high barrier to resistance. *Antimicrob Agents Chemother*. 2022;66(7):e0019822. doi:10.1128/aac.00198-22
18. Heyer A, Gunther T, Robitaille A, et al. Remdesivir-induced emergence of SARS-CoV2 variants in patients with prolonged infection. *Cell Rep Med*. 2022;3(9):100735. doi:10.1016/j.xcrm.2022.100735
19. Gandhi S, Klein J, Robertson AJ, et al. De novo emergence of a remdesivir resistance mutation during treatment of persistent SARS-CoV-2 infection in an immunocompromised patient: a case report. *Nat Commun*. 2022;13(1):1547. doi:10.1038/s41467-022-29104-y
20. N'Guessan A, Kailasam S, Mostefai F, et al. Selection for immune evasion in SARS-CoV-2 revealed by high-resolution epitope mapping combined with genome sequence analysis. *biorxiv*. 2022. doi:10.1101/2022.06.01.494373
21. Mishra D, Suri GS, Kaur G, Tiwari M. Comparative insight into the genomic landscape of SARS-CoV-2 and identification of mutations associated with the origin of infection and diversity. *J Med Virol*. 2021;93(4):2406–2419. doi:10.1002/jmv.26744
22. Wu C, Qavi AJ, Hachim A, et al. Characterization of SARS-CoV-2 nucleocapsid protein reveals multiple functional consequences of the C-terminal domain. *iScience*. 2021;24(6):102681. doi:10.1016/j.isci.2021.102681